Journal of Power Sources 196 (2011) 2669–2675

Contents lists available at ScienceDirect

Journal of Power Sources

journal homepage: www.elsevier.com/locate/jpowsour

Low methanol crossover and high efficiency direct methanol fuel cell: The influence of diffusion layers

A. Casalegno[a,*], C. Santoro[b], F. Rinaldi[a], R. Marchesi[a]

[a] Department of Energy, Politecnico di Milano, Via Lambruschini 4, 20156 Milano, Italy
[b] Department of Civil and Environmental Engineering, University of Connecticut, United States

ARTICLE INFO

Article history:
Received 20 September 2010
Received in revised form 18 October 2010
Accepted 7 November 2010
Available online 12 November 2010

Keywords:
DMFC
Methanol crossover
Diffusion layer
Experiment

ABSTRACT

This experimental work aims to investigate the possibility to reduce methanol crossover in DMFC modifying diffusion layer characteristics. Improvements in crossover measurement are firstly proposed, permitting to conclude that in the investigated conditions carbon dioxide flow through the membrane can be neglected. The experimental results evidence that introducing appropriate anode and cathode microporous layers determines: a strong reduction in methanol crossover, approximately 45% at low current density; a considerable increment of efficiency; a moderate decrease of power density. The complete experimental analysis demonstrates that methanol transport in both liquid and vapour phases can be controlled modifying properly diffusion layer characteristics in order to increase DMFC efficiency.

1. Introduction

Hydrogen polymer electrolyte membrane fuel cell (PEMFC) is considered a highly promising technology, especially for micro-power generation and vehicular applications, due to its important attributes: low temperature and low pressure operation, no liquid electrolyte, high power density. The direct methanol fuel cell (DMFC) technology is a further development of PEMFC. Its most promising applications are portable electronics and the automotive industry, thanks to the direct use of a high energy density liquid fuel [1]. However, the fuel is also the cause of its main drawbacks: lower efficiency and lower power density than PEMFC. This is due to methanol permeation through the polymer membrane and the slower electrochemical methanol oxidation [2]. Methanol crossover is defined as the permeation of methanol through the electrolyte membrane. State of the art membranes used in PEMFC are not fully impermeable to methanol and allow for significant quantities to permeate from the anode to the cathode [3]. Diffusion and electro-osmotic drag are the two key mechanisms identified. When methanol reaches the cathode it is oxidized, leading to a mixed potential and an inevitable decrease in cell voltage. Moreover the oxidized methanol is effectively wasted fuel with clear negative impact in the overall efficiency of the cell. Methanol crossover in DMFC has been extensively studied both experimentally and theoretically, elucidating its dependence on operating conditions and diffusion layers (GDL) characteristics [4–12]. Despite the crucial role of these components on mass transport, the investigations on GDL aim generally to evaluate directly their influence on performance; in literature the most analyzed GDL characteristics are: morphology, thickness, and PTFE content [13–16], presence of hydrophobic microporous layer (MPL) at cathode side [14,17–21], presence of hydrophobic or hydrophilic MPL at anode side [15,17,21–24]. Some of these works report also measurements of water transport through the membrane electrode assembly (MEA); they focus in reducing water transfer, mainly to permit high methanol concentration feeding, through different GDL optimization strategies [12,14,17–21,23,25]. Methanol crossover measurements are generally neglected, just few works report qualitative and limited analyses [17,20,26]; the literature lacks of accurate and quantitative analyses regarding the influence of GDL properties on methanol crossover. The mechanisms that regulate methanol transport through anode GDL in DMFC are not fully understood yet, due to the complicate two-phase, multicomponent transport phenomena through porous media, and the potential of reducing methanol crossover through GDL modification is not completely explored.

In previous works [27,28] the authors presented systematic and accurate investigations of methanol crossover varying operating conditions in wide ranges. The obtained results evidence the possibility to reduce crossover decreasing liquid methanol concentration in the anode electrode, taking advantage of vapour methanol transport for the electrochemical reaction.

This work aims to analyze this possibility adopting appropriate anode and cathode GDL. In fact these components may be opti-

* Corresponding author. Tel.: +39 0223993912; fax: +39 0223993912.
E-mail address: andrea.casalegno@polimi.it (A. Casalegno).

0378-7753/$ – see front matter © 2010 Elsevier B.V. All rights reserved.
doi:10.1016/j.jpowsour.2010.11.050

Nomenclature

η	efficiency
F	Faraday constant [=96,500 C mol^{-1}]
I	electrical current [A]
i	electrical current density [A cm^{-2}]
LHV	low heating value [J mol^{-1}]
m	mass flow rate [g min^{-1}]
N	molar flow rate [mol s^{-1}]
n	specific molar flow rate [mol s^{-1} cm^{-2}]
P	pressure [kPa]
T	temperature [K]
u	measurement uncertainty [variable]
V	fuel cell voltage [V]
X	molar or mass fraction [% or wt.%]

Subscripts

air	relative to air
CH_3OH	relative to methanol
CO_2	relative to carbon dioxide
(g)	relative to vapour phase
H_2O	relative to water
O_2	relative to oxygen
tot	relative to total flow

Superscripts

a	at anode
c	at cathode
cons	consumed at the electrode
crossover	relative to crossover
in	at inlet
mem	transported through the membrane
out	at outlet

mized, eventually introducing microporous layers (MPLs), in order to control methanol and water transport through the MEA in both liquid and vapour phases.

In the present manuscript an accurate experimental characterization of DMFC performance and methanol crossover with different GDL is presented. Moreover some improvements in crossover measurement are proposed, to evaluate accurately the debated contribution of CO_2 flow through the membrane electrode assembly (MEA), from anode to cathode, reported in literature [3,10] and to analyze the minor effects of cathode feeding on crossover, not exhaustively investigated in literature, due to less accurate experimental methodologies.

2. Methodology

2.1. Carbon conservation analysis

In the following section a carbon conservation analysis is reported in order to describe the methodology applied to estimate methanol crossover from measurement data.

Methanol flow rate at anode outlet depends on the flux converted by the electrochemical reaction and crossover, as expressed in the following equations:

$$N_{CH_3OH}^{a,out} = N_{CH_3OH}^{a,in} - N_{CH_3OH}^{a,cons} - N_{CH_3OH}^{crossover} \quad (1)$$

$$N_{CH_3OH}^{a,cons} = \frac{I}{6F} \quad (2)$$

Gas phase flow rate at anode outlet is composed of the contributes of carbon dioxide, methanol and water[1]:

$$N_{tot(g)}^{a,out} = N_{CO_2}^{a,out} + N_{H_2O(g)}^{a,out} + N_{CH_3OH(g)}^{a,out} \quad (3)$$

Carbon dioxide flow rate at anode outlet depends on the electrochemical reaction rate and CO_2 flow through the membrane:

$$N_{CO_2}^{a,out} = \frac{I}{6F} - N_{CO_2}^{mem} \quad (4)$$

Consequently CO_2 flow through the membrane can be estimated measuring properly gas phase flow rate at anode outlet.

Assuming complete methanol oxidation at cathode side [3], methanol crossover is equal to CO_2 flow rate at cathode outlet subtracted by CO_2 flow through the membrane and CO_2 flow rate at cathode inlet, due to ambient concentration:

$$N_{CH_3OH}^{crossover} = N_{CO_2}^{crossover} = N_{CO_2}^{c,out} - N_{CO_2}^{mem} - N_{CO_2}^{c,in} \quad (5)$$

CO_2 flow rate at cathode outlet can be estimated measuring CO_2 fraction at cathode outlet, where total flow rate depends on: air inlet, O_2 consumption (due to electrochemical reaction and crossover methanol oxidation), water flow[1], methanol crossover, CO_2 flow through the membrane, as expressed in:

$$N_{CO_2}^{c,out} = X_{CO_2}^{c,out} \cdot N_{tot}^{c,out} \quad (6)$$

$$N_{tot}^{c,out} = N_{air}^{c,in} - N_{O_2}^{c,cons} + N_{H_2O}^{c,out} + N_{CO_2}^{crossover} + N_{CO_2}^{mem} \quad (7)$$

$$N_{O_2}^{c,cons} = \frac{I}{4F} + \frac{3}{2} \cdot N_{CO_2}^{crossover} \quad (8)$$

The contributions of water production, oxygen consumption and CO_2 flow through the membrane can affect dramatically methanol crossover estimation, thus they have to be carefully considered.

2.2. Experimental equipment and measurement uncertainty

The experimental analyses of DMFC performance and methanol crossover are carried out utilizing the same equipment and methodologies presented in [28], that permit to evaluate measurement uncertainty and to verity reproducibility, except the following integrations.

Cathode side is modified introducing, Fig. 1:

- a condenser and a liquid separator before CO_2 fraction measurement (uncertainty 2% + 200 ppm);
- a thermocouple (uncertainty 0.2 °C) in the CO_2 sensor vessel.

Water concentration in the CO_2 sensor vessel has been measured for different conditions with a VAISALA HMT333 humidity sensor, prior to the experimental campaign: water concentration can be estimated with good agreement approximating saturation at thermocouple temperature (very close to ambient temperature).

Thus these modifications permit to measure water fraction in CO_2 sensor vessel and consequently $N_{H_2O}^{c,out} = X_{H_2O}^{c} \cdot N_{tot}^{c,out}$.[2]

The introduction of these components do not alter the transitory time necessary to reach steady state in the vessel: the sum of condenser, liquid separator and vessel volumes is approximately

[1] Water and methanol flows in gas phase can be minimized cooling down the gas mixture near to ambient temperature, then water and methanol fractions can be estimated in condensing conditions. Methanol flow rate in gas phase near ambient temperature is negligible in comparison to the other terms.

[2] Carbon dioxide dissolved in liquid water at both anode and cathode sides has been estimated: it is negligible, because it is more than 1 order of magnitude inferior than the amount remaining in the gas phase.

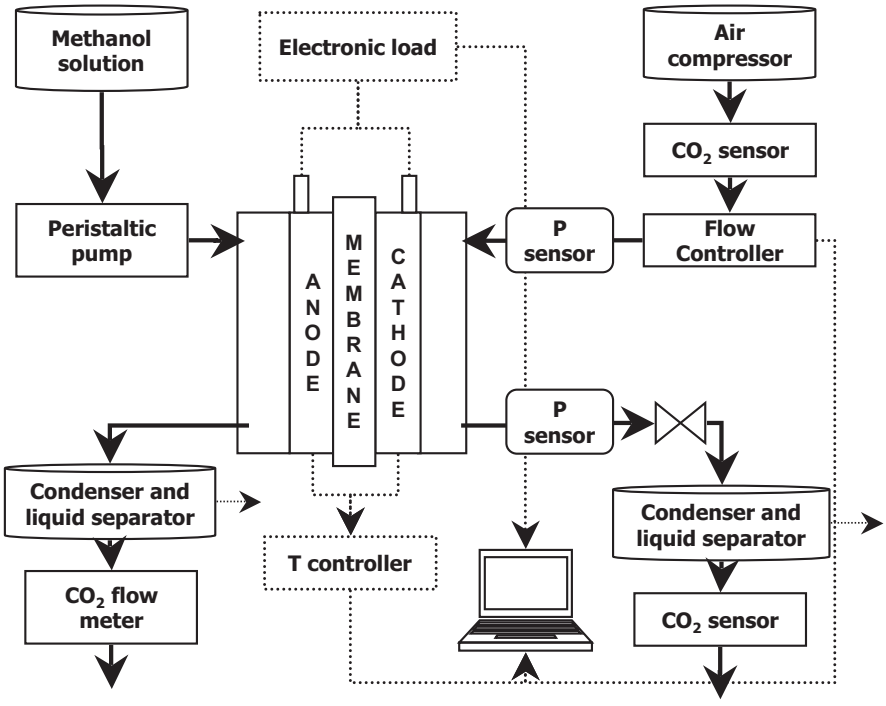

Fig. 1. Experimental setup scheme.

250 cm^3, included between one fifth and one tenth of the gas volume flowing during the 400 s acquisition at constant condition. In fact the initial transitory to reach CO_2 concentration steady state condition last 50–100 s.

Anode side is modified introducing:

- a condenser and a liquid separator with a thermocouple (uncertainty 0.2 °C);
- a CO_2 calibrated flow meter (uncertainty 0.7% + 0.4 N cm^3 min^{-1}).

As previously described for CO_2 sensor vessel, water concentration just before CO_2 flow meter has been measured for different conditions: water concentration can be estimated with good agreement approximating saturation at thermocouple temperature (very close to ambient temperature).

Anode CO_2 flow rate measures are corrected considering estimated water content ($N^{a,out}_{H_2O(g)}$).

CO_2 flow from anode to cathode ($N^{mem}_{CO_2}$) is evaluated comparing anode CO_2 flow rate ($N^{a,out}_{CO_2}$) with the theoretical production.

The investigated conditions of the experimental analysis are reported in Table 1.

The uncertainty associated with the measurement of current density is evaluated according to [29]. The contribution of each controlled parameter is assessed considering the uncertainty of each measuring device and estimating experimentally its impact on the current measurement. The final and total uncertainty associated with the current measurement is equal to the geometric sum of the uncertainties of each controlled parameter. The uncertainty, u_i (179 dof, 95% population) for current density, specific to fuel cell active area, i from 0 to 0.6 A cm^{-2}, is estimated equal to:

$$u_i = -5 \times 10^{-2} \cdot i^2 + 2.5 \times 10^{-2} \cdot i + 3.3 \times 10^{-3} \text{ A cm}^{-2} \quad (9)$$

A similar methodology is applied to evaluate methanol crossover uncertainty. Considering operating conditions influence the uncertainty, $u_{crossover}$ (179 dof, 95% population), of methanol crossover flux, specific to fuel cell active area, $n^{crossover}_{CH_3OH}$ from 0 to 7×10^{-7} mol s^{-1} cm^{-2} is estimated equal to:

$$u_{crossover} = 2.3\% \cdot n^{crossover}_{CH_3OH} + 1.1 \times 10^{-8} \text{ mol s}^{-1}\text{cm}^{-2} \quad (10)$$

The catalyst-coated membranes (CCM) used in this work are commercial; their active area is 22.1 cm^2. The membrane is Nafion-117, anode catalysed layer presents a metal loading of 2 mg cm^{-2} (Pt:Ru = 2 wt.%), cathode catalysed layer presents a metal loading of 1.3 mg cm^{-2} (Pt). The investigated GDL for both anode and cathode are commercial; the characteristics are reported in Table 2. Cell gaskets consist in a Mylar layer (thickness 50 mm), in contact with the membrane, and a fibreglass layer covered by PTFE (thickness 250 mm). The MEA are identified as following: MEA GG, GDL without MPL on both anode and cathode; MEA MM, GDL with MPL on both sides, MEA GM, GDL without MPL at anode and GDL with MPL at cathode.

Table 1
Investigated operating conditions.

Controlled parameter	Investigated range	Uncertainty
Voltage (V)	0.1–0.6 V	0.5% + 1 mV
Fuel cell temperature (T)	333–353 K	0.05 K
Methanol mass fraction (X)	3.25–6.5% wt.	0.07% wt.
Anode flow rate (m_{met})	1 g min^{-1}	1%
Anode mean pressure (P_a)	101 kPa	5 kPa
Air flow rate (m_{air})	0.62–1.14 g min^{-1}	0.7% + 0.005 g min^{-1}
Cathode mean pressure[a] (P_c)	115–150 kPa	5 kPa

[a] Cathode mean pressure is calculated as the mean value between inlet and outlet pressures.

3. Results

3.1. CO_2 flow through membrane

Carbon dioxide flow through the membrane is measured for every investigated condition, as previously described. The differences in respect to theoretical production are minor than measurement uncertainty in 90% of the cases (magnitude order 10^{-8} mol s^{-1} cm^{-2}); the analysis of variance confirmed that the dif-

Table 2
GDL characteristics.

Name	Thickness (μm)	PTFE content	Areal weight (g m^{-2})	Air permeability (cm^3 cm^{-2} s^{-1})	Electrical resistance (Ω cm^2)
GDL with MPL	415	10%	145	1.45	<18
GDL without MPL	400	10%	90	85	<14

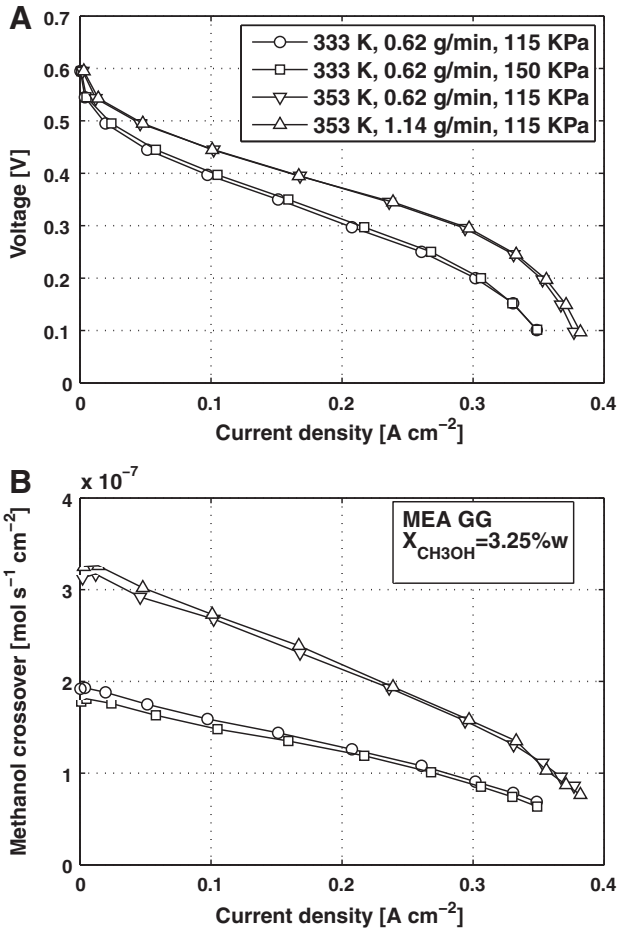

Fig. 2. Polarization curve (A) and methanol crossover (B) varying, temperature, air flow rate and cathode pressure, MEA GG, $X_{CH_3OH} = 3.25$ wt%.

ferences are not statistically significant.[3] Thus CO_2 flow through the membrane can be considered negligible. Consequently Eqs. (4), (5) and (7) can be simplified, eliminating the term $N_{CO_2}^{mem}$.

Finally the results confirm that CO_2 measurement at cathode outlet in the investigated ranges, if properly carried out, is a reliable indicator of methanol crossover. CO_2 flow measured in some works in literature could be determined by peculiar operating conditions or materials, anode over-pressure or internal leakages.

3.2. Cathode feeding influence

The experimental results, regarding methanol feeding effect on methanol crossover, are coherent with the interpretation presented in [28], thus they are not reported in the following.

In this work cathode feeding influence on crossover is evaluated. In Fig. 2 performance and methanol crossover curves are reported, varying air flow rate and cathode mean pressure. In these cases performances are limited by anode feeding, because of the low methanol fraction. Coherently an increase in oxygen partial pressure at cathode, effectuated raising air flow or cathode pressure, does not affect considerably performances. These minimal positive variations have the same magnitude than measurement uncertainty.

Increasing air flow rate and cathode pressure has a very limited influence on methanol crossover. The variations again have the magnitude order of measurement uncertainty. Generally in the investigated conditions a pressure increase determines a slight crossover reduction, while an air flow increase has an opposite effect. The reason is probably correlated to water transport: an increase in water transport through the MEA, due to air flow increase or pressure reduction, may determine an increase in methanol transport, through different mechanisms [12,14,18], affecting also methanol concentration at anode side. Further experimental work is necessary to investigate these phenomena.

At higher methanol fraction, Fig. 3, the performances are not anymore limited by anode feeding, but they are considerably affected by a higher crossover. In these cases an increase of cathode pressure enhances performance in the whole current density range, improving cathode kinetics, while an increase of air flow has

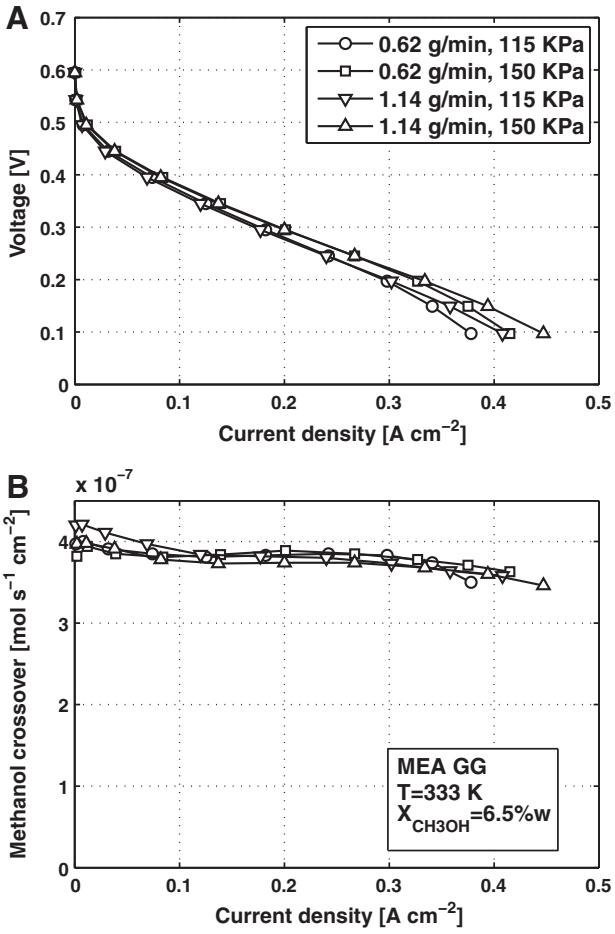

Fig. 3. Polarization curve (A) and methanol crossover (B) varying air flow rate and cathode pressure, MEA GG, X_{CH_3OH}: 6.5 wt.%, T: 333 K.

[3] A comparison of measure and theoretical values is reported in the supplementary material.

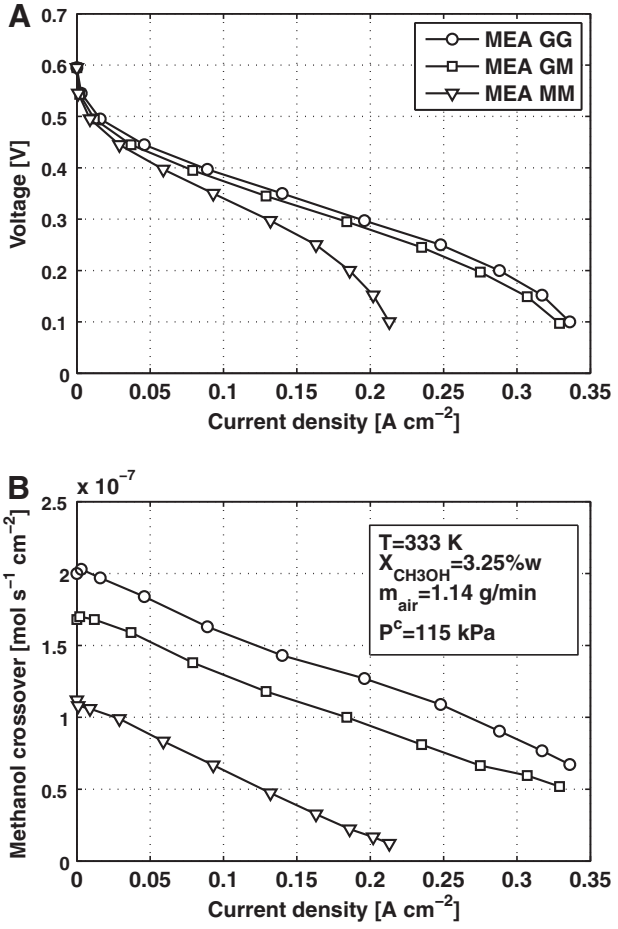

Fig. 4. Polarization curve (A) and methanol crossover (B) for different MEA, X_{CH_3OH}: 3.25 wt.%, T: 333 K, m_{air}: 1.14 g min^{-1}, P^c: 115 kPa.

an effect only at high current density, improving oxygen transport to the electrode.

These variations in cathode feeding still have a very small effect on methanol crossover, whose changes are again comparable to measurement uncertainty and coherent with the previous comments. It is worth noticing that in the investigated conditions oxygen stoichiometry, considering the consumption of both the electrochemical reaction and crossover oxidation, is always higher than 2. Thus oxygen availability is never strongly limited, permitting the complete oxidation of methanol at cathode, due to crossover; in these conditions the adopted crossover measurement methodology is reliable. Consequently in the investigated conditions cathode feeding has very modest effects on methanol crossover and its measurement.

3.3. Diffusion layers influence

The general influence of operating conditions, including cathode pressure and air flow, on performance and crossover, is confirmed for all MEA, thus it will not be discussed in details.

The effects of introducing MPL at anode and cathode sides on performance and crossover are reported in Fig. 4. The presence of MPL at cathode (MEA GM) does not affect substantially the performance: there is a modest reduction, probably due to a decrease of mass transport coefficient, which worsens cathode kinetics. The MPL determines instead a strong reduction in methanol crossover, approximately 15% at open circuit voltage (OCV): as reported in literature [12,14,17,18] this layer decreases water transport through the MEA, especially in liquid phase, implying a similar reduction

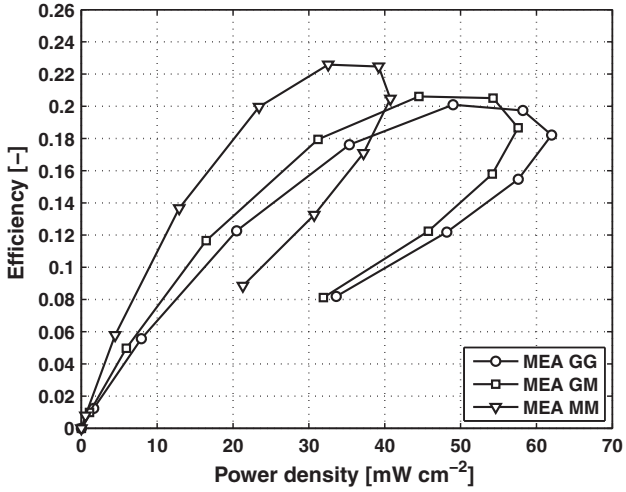

Fig. 5. Efficiency in function of power density for different MEA, X_{CH_3OH}: 3.25 wt.%, T: 333 K, m_{air}: 1.14 g min^{-1}, P^c: 115 kPa.

in methanol transport. The crossover reduction remains approximately constant in the whole current range and it is clearly evident also at very low current density, where the major transport mechanism through the membrane is diffusion, confirming that liquid methanol concentration in the anode electrode is lowered by MPL presence.

Introducing also an MPL at anode side (MEA MM) the performances are strongly reduced by an evident limitation in methanol availability. The MPL characteristics hinder the transport of liquid methanol–water solution, reducing methanol concentration in the electrode. This effect has a dramatic influence on methanol crossover: a reduction of approximately 45% at OCV compared to MEA GG.

To compare more accurately the MEA two further quantities can be utilized: power density, that affects the investment cost, and efficiency, that determines fuel consumption, direct cost. Efficiency is defined considering exhaust fuel recirculation [28]:

$$\eta = \frac{VI}{[(N^{a,cons}_{CH_3OH} + N^{crossover}_{CH_3OH})LHV]} \quad (11)$$

where converted fuel flow includes the fractions used in the electrochemical reaction and wasted with methanol crossover.

The efficiency of the three MEA in function of power density is reported in Fig. 5. The introduction of MPL in MEA GM and MEA MM determines in general an increment in the efficiency but also a reduction in power density. In fact, as previously discussed, crossover reduction is accompanied by performance decreasing. The maximum efficiencies achieved by MEA MM, GM and GG respectively are 22% at 38 mW cm^{-2}, 21% at 50 mW cm^{-2}, 20% at 54 mW cm^{-2}. At lower power density the increase in the efficiency, due to crossover reduction, is still more effective: halving power density the efficiencies are 17% at 19 mW cm^{-2}, 16% at 25 mW cm^{-2}, 15% at 27 mW cm^{-2}. Depending on the effective application and operation, the requirements on efficiency or power density may vary significantly; therefore components and operating conditions have to be optimized for each specific case. The present analysis does not pretend to individuate an optimal GDL configuration for a certain application but to demonstrate that GDL can be modified to improve DMFC efficiency, suffering a power density reduction.

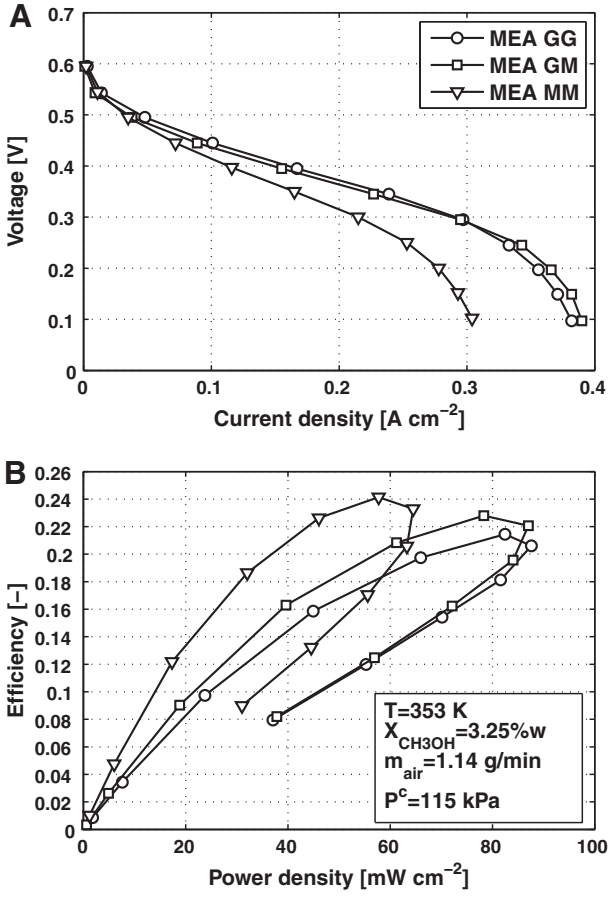

Fig. 6. Polarization curve (A) and efficiency (B) for different MEA, X_{CH_3OH}: 3.25 wt.%, T: 353 K, m_{air}: 1.14 g min^{-1}, P^c: 115 kPa.

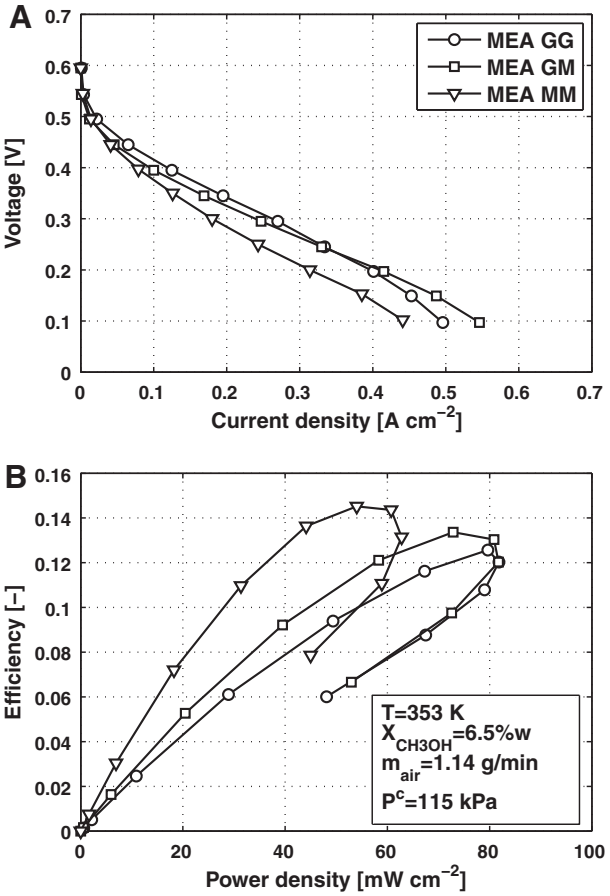

Fig. 7. Polarization curve (A) and efficiency (B) for different MEA, X_{CH_3OH}: 6.5 wt.%, T: 353 K, m_{air}: 1.14 g min^{-1}, P^c: 115 kPa.

Comparing the three MEA at 353 K, Fig. 6, the results are similar: methanol crossover reductions have the same entities,[4] instead performance decreases are less evident.

The higher temperature permits higher methanol concentration and transport in vapour phase [28], reducing the difference between the maximum current densities of MEA MM and MEA GG from 35% to 20%. Methanol crossover reductions are instead analogous: 15% at OCV comparing MEA GM and MEA GG, 45% comparing MEA MM and MEA GG. Also in this case the differences are constant in the whole current range, except at very high current. These results substantiate the possibility to reduce crossover decreasing liquid methanol concentration in the anode electrode, taking advantage of vapour methanol transport for the electrochemical reaction.

At higher temperature the increment in efficiency, introducing MPL, is still more evident, Fig. 6, accompanied by a lower power density reduction, thanks to the enhanced methanol transport in vapour phase. The maximum efficiencies achieved by MEA MM, GM and GG respectively are 24% at 62 mW cm^{-2}, 23% at 80 mW cm^{-2}, 22% at 82 mW cm^{-2}.

At double methanol fraction the performance are not anymore limited by anode feeding, Fig. 7. MEA GM, compared to MEA GG, demonstrates worse performance at low current density in spite of lower crossover, again a 15% reduction at OCV. This is mainly caused by lower oxygen availability at cathode, determined by increased mass transport resistance due to MPL presence, on the contrary at high current MPL reduces flooding effect and permits better performance [12,14,16,30]. The MEA MM performances are inferior to MEA GM and GG ones; the differences may be attributed mainly to a worse membrane hydration: anode MPL reduces both methanol and water transport to the membrane, as already stated. Comparing with the case of lower methanol concentration feeding, Fig. 6, this reduction in performance is lower. Methanol crossover reduction remains instead unaltered at OCV, as in previous comparisons around 45%. This is a further confirmation that the effective methanol concentration in the anode electrode is reduced by MPL. This trend furthermore determines a higher improvement in efficiency, thanks to anode MPL, compared to previous results.

In order to confirm the origin of MEA MM worse performance, experimental results at lower air flow rate are reported in Fig. 8; methanol crossover is not significantly affected by air flow variation.

With a diminished air flow MEA GG presents lower performance, due to lower oxygen availability, especially at high current density; the reduction in MEA GM performance is still worse, because of the increased mass transport resistance due to MPL presence. MEA MM instead performs slightly better, thanks mainly to a better membrane hydration, as supposed. Water transport is modified by anode MPL presence: flooding effect is still very limited, compare to other MEA, permitting high oxygen availability and current density. Further experimental work is necessary to characterize accurately the anode MPL influence on water transport through DMFC.

The positive increment in MEA MM performance at constant methanol crossover determines an enhanced efficiency, while MEA GG and GM present an efficiency reduction, evidencing the effec-

[4] The methanol crossover data relative to the following analysis are reported in the supplementary material.

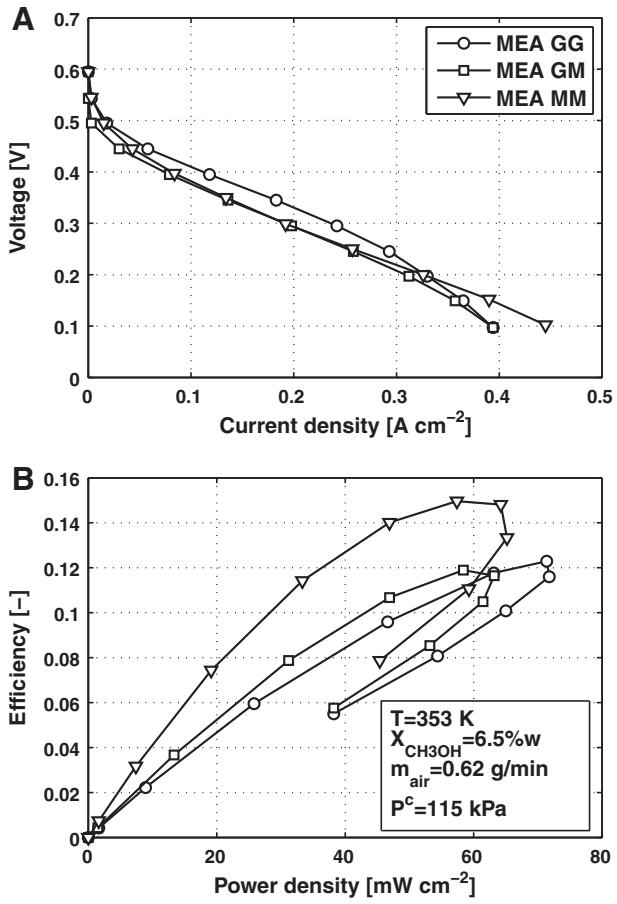

Fig. 8. Polarization curve (A) and efficiency (B) for different MEA, X_{CH_3OH}: 6.5 wt.%, T: 353 K, m_{air}: 0.62 g min^{-1}, P^c: 115 kPa.

tiveness of limiting methanol crossover through a combined GDL and operating conditions optimization.

4. Conclusions

The experimental characterization of DMFC performance and methanol crossover with different diffusion layers presented in the manuscript permits to draw the following conclusions:

- carbon dioxide flow through the membrane, measured for every investigated condition, can be considered negligible; CO_2 measurement at cathode outlet, if properly carried out, is a reliable indicator of methanol crossover;
- in the investigated conditions cathode feeding has very slight effects on methanol crossover: a pressure increase determines a minor crossover reduction, while an air flow increase has an opposite effect; the reason is correlated to water transport;
- the presence of cathode MPL has minor effects on performance; it determines a strong reduction in methanol crossover, approximately 15% at low current density: this layer decreases water transport through the MEA, especially in liquid phase, implying a similar reduction in methanol transport;
- introducing an anode MPL, both methanol and water transport through the membrane are strongly affected: at low methanol concentration the performances are limited by low methanol availability, at higher methanol concentration a worse membrane hydration may reduce performance; the anode MPL also has a dramatic influence on methanol crossover: a reduction of approximately 45% at low current density;
- the introduction of MPL at both anode and cathode determines in general a considerable increment in the efficiency but also a moderate decrease of power density;
- methanol crossover can be reduced modifying GDL characteristics to decrease liquid methanol concentration in the anode electrode, taking advantage of vapour methanol transport for the electrochemical reaction; the effectiveness of this strategy can be maximized combining GDL characteristics and operating conditions optimization.

Acknowledgement

Funding for this work from Fondazione Cariplo under agreement no. 2007.5543 is acknowledged.

Appendix A. Supplementary data

Supplementary data associated with this article can be found, in the online version, at doi:10.1016/j.jpowsour.2010.11.050.

References

[1] A.S. Aricò, S. Srinivasan, V. Antonucci, Fuel Cells 1 (2001) 133–161.
[2] A. Heinzel, V.M. Barragan, Journal of Power Sources 84 (1999) 70–74.
[3] H. Dohle, J. Divisek, J. Mergel, H.F. Oetjen, C. Zingler, D. Stolten, Journal of Power Sources 105 (2002) 274–282.
[4] X. Ren, P. Zelenay, S. Thomas, J. Davey, S. Gottesfeld, Journal of Power Sources 86 (2000) 111–116.
[5] S. Eccarius, B.L. Garcia, C. Hebling, J.W. Weidner, Journal of Power Sources 179 (2008) 723–733.
[6] S.H. Seo, C.S. Lee, Applied Energy 87 (2010) 2597–2604.
[7] T. Schultz, K. Sundmacher, Journal of Membrane Science 276 (2006) 272–285.
[8] T.S. Zhao, C. Xu, R. Chen, W.W. Yang, Electrochimica Acta 52 (2007) 5266–5271.
[9] K. Sundmacher, K. Scott, Chemical Engineering Science 54 (1999) 2927–2936.
[10] R.Z. Jiang, D.R. Chu, Journal of Electrochemical Society 151 (2004) A69–A76.
[11] T.S. Zhao, C. Xu, R. Chen, W.W. Yang, Progress in Energy and Combustion Science 35 (2009) 275–292.
[12] C. Xu, T.S. Zhao, Journal of Power Sources 168 (2007) 143–153.
[13] B. Krishnamurthy, S. Deepalochani, Journal of Hydrogen Energy 34 (2009) 446–452.
[14] C. Xu, T.S. Zhao, Y.L. He, Journal of Power Sources 171 (2007) 268–274.
[15] J. Zhang, G.P. Yin, Q.Z. Lai, Z.B. Wang, K.D. Cai, P. Liu, Journal of Power Sources 168 (2007) 453–458.
[16] C. Xu, T.S. Zhao, Q. Ye, Electrochimica Acta 51 (2006) 5524–5531.
[17] F. Liu, G. Lu, C.Y. Wang, Journal of Electrochemical Society 153 (2006) A543.
[18] G.Q. Lu, F.Q. Liu, C.Y. Wang, Electrochemical Solid-State Letter 8 (2005) A1.
[19] J. Cao, M. Chen, J. Chen, S. Wanga, Z. Zou, Z. Li, D.L. Akins, H. Yang, Journal of Hydrogen Energy 35 (2009) 4622–4629.
[20] C. Xu, A. Faghri, X. Li, T. Ward, Journal of Hydrogen Energy 35 (2010) 1769–1777.
[21] F. Liu, C.Y. Wang, Electrochimica Acta 53 (2008) 5517–5522.
[22] J. Li, D.D. Ye, X. Zhu, Q. Liao, Y.D. Ding, X. Tian, Journal Applied Electrochemistry 39 (2009) 1771–1778.
[23] Q.X. Wu, T.S. Zhao, R. Chen, W.W. Yang, Journal of Power Sources 191 (2009) 304–311.
[24] S.H. Yanga, C.Y. Chen, W.J. Wanga, Journal of Power Sources 195 (2010) 3536–3545.
[25] Y.H. Pan, Journal of Power Sources 161 (2006) 282–289.
[26] G.Q. Lu, C.Y. Wang, Journal of Fuel Cell Science and Technology 3 (2006) 131–136.
[27] A. Casalegno, P. Grassini, R. Marchesi, Applied Thermal Engineering 27 (2007) 748–754.
[28] A. Casalegno, R. Marchesi, Journal of Power Sources 185 (2008) 318–330.
[29] Env 13005 1999, BIPM, IEC, IFCC, ISO, IUPAC, IUPAP, OIML, International Organization for Standardization, 1993 (ISBN 92-67-10188-9).
[30] A. Casalegno, L. Colombo, S. Galbiati, R. Marchesi, Journal of Power Sources 195 (2010) 4143–4148.